Published in Applied Energy 2022; 328: 120257. 10.1016/j.apenergy.2022.120257

Day-ahead Scheduling of 100% Isolated Communities under Uncertainties through a Novel Stochastic-Robust model

Marcos Tostado-Véliz[1], Ahmad Rezaee Jordehi[2], Seyed Amir Mansouri[3], Francisco Jurado[1],*

1. Department of Electrical Engineering, University of Jaén, Linares 23700 (e-mail: mtostado@ujaen.es (M.T.-V.), fjurado@ujaen.es (F.J.)).
2. Department of Electrical Engineering, Rasht Branch, Islamic Azad University, Rasht 43, Iran (e-mail: ahmadrezaeejordehi@gmail.com).
3. Department of Electrical Engineering, Yadegar-e-Imam Khomeini (RAH) Share Rey Branch, Islamic Azad University, Tehran, Iran (e-mail: amir.mansouri24@gmail.com).

* Correspondence: fjurado@ujaen.es.

Abstract. Energy communities enable effective coordination among prosumers on pursuing collective targets. This paper focuses on isolated 100% renewable communities, involving individual (controllable appliances and small generators) and collective (wind generators and battery banks) assets. To effectively coordinate the agents involved in these structures, advanced energy management strategies are necessary. This work develops a three-stage day-ahead scheduling strategy for isolated 100% energy communities, involving peer-to-peer transactions among prosumers. The different uncertainties involved are incorporated through a novel stochastic-robust formulation, that results in a computationally tractable optimization framework. To validate the new model, a case study on a six-prosumer benchmark community is analysed. Results reveal the importance of collective assets and peer-to-peer exchanges among prosumers as well as the effectiveness of the developed formulation. The role of batteries is also discussed, helping to reduce the total unserved energy and operating cost by 20% and 19%, respectively, as well as enabling a more efficient use of wind energy. The impact of robustness is also studied, incrementing the expected importable energy by 28% compared to the deterministic case, while the exportable energy from prosumers is notably reduced by 40%. However, uncertainty-aware strategies have a direct impact on operational costs, incrementing the expenditures by 37% when uncertainties are considered.

Keywords. Energy community; Energy storage; Peer-to-peer; Photovoltaic; Renewable energy; Robust optimization; Stochastic programming; Wind energy.

Nomenclature

Indexes (Sets)	
$i, j(Q)$	Prosumer
$t(T)$	Time
$a\left(A^{i}_{NI/I}\right)$	i^{th} customer-owned controllable appliance (NI: non-interruptible, I: interruptible)
$s(S)$	Scenario
$r(R)$	Representative scenario
Θ	Allowable time window
Ω	Cluster of a representative scenario

Superscripts	
pur / exp	Importable/exportable
PV	Photovoltaic
NC	Non-controllable
$air, in / out$	Indoor/outdoor air
$build$	Building or dwelling
$HVAC, h / c$	Heating-ventilation-air conditioner system in heating/cooling mode
$W, h / c$	Hot/cold water
EWH	Electric water heater
sp / db	Setpoint/deadband
EC	It refers to collective assets owned by the community
$BES, ch / dch$	Battery energy storage in charging/discharging mode
WG	Wind generator
NS	Non-served

Functions	
$\mathrm{E}(\bullet)$	Expected value
$\mathrm{size}(\bullet)$	Number of elements within a set or vector
$\underline{(\bullet)} / \overline{(\bullet)}$	Minimum/maximum value

Parameters & constants	
ϑ	Solar irradiance (kW/m²)
θ	Temperature (ºC or K)
η	Efficiency (%)
$\Delta\tau$	Time step (h)
δ	Duty cycle (h)
m	Mass (kg)

C	Heat or thermal capacity ($kJ \cdot kg^{-1} \cdot {}^{o}C^{-1}$ or $kWh \cdot {}^{o}C^{-1}$)
R	Equivalent thermal resistance ($kW \cdot {}^{o}C^{-1}$)
COP	Coefficient of performance (p.u.)
v	Volume (gal or m^3)
ω	Probability (%)
μ	Maintenance cost (\$/kWh or \$/kWh^2)
Γ	Robust parameter (-)
e2P	Energy-to-power ratio (h)
DOD	Depth of discharge (%)
γ	Wind speed (m/s)
α , β	Coefficients of wind turbine ($kW \cdot (m/s)^{-3}$, -)
λ	Energy cost (\$/kWh)

Decision variables

p	Power (kW)
π	Commitment status (binary)
ε	Energy (kWh)
on / off	ON/OFF status (binary)
z , q , y	Auxiliary variables for robust representation (-)

1 - Introduction

1.1 - Context and motivation

Nowadays, existing power networks are facing several problems concerned to their reliability and pollution [1-3], which are principally caused by an increasing demand observed during the last decade [4, 5], especially due to an increment in the use of air conditioner systems [6]. Higher penetration of renewable sources as well as deployment of distributed energy storage systems, may help to partially alleviate such issues [7-9]. However, several concerns arise regarding the coordination and management of such resources in isolated systems, where the weakness of existing infrastructures may suppose a critical problem [10].

Regarding the inclusion of new renewable sources and storage systems, this emerging framework motivates the development of new paradigms and businesses, which are evolving from traditional centralized systems to decentralized ones, which encourage the active participation of end users [11]. In such context, energy communities (ECs) have emerged as a valuable paradigm to locally coordinating the available resources on pursuing the maximization of collective welfare [12]. There is a variety of definitions for ECs; nevertheless, the most extended is that provided in [13], where an EC is defined as an aggregation of multiple users, traditionally consumers or prosumers.

Therefore, it results clear that ECs may suppose a valuable contribution to increase the penetration of renewable generators and thus boosting up the efficiency of electricity systems, but also for enabling access to electricity supply in remote and rural areas, where difficulties in extending existing networks make almost impossible energy supply. This is a critical issue since, even nowadays, more than 770 million live without access to electricity, mostly in Africa and Asia [14]. In such context, ECs may help to coordinate

prosumers, who can share resources as well as take advantage of collective assets, such as large generators or storage systems, which are difficult to install individually [15].

For the effective coordination of the agents involved in community operation, energy management tools are essential, especially under uncertain environments caused by intermittent renewable generation and unpredictable demand [16]. The importance of ECs in future energy systems motivate to develop specific tools suitable for such systems, which must account for peer-to-peer (P2P) energy transactions among prosumers and other particularities [17, 18]. This work focuses on this topic.

1.2 - Related works

This paper focuses on energy management in ECs. The state-of-the-art about this topic is still quite narrow, especially if compared with other similar topics. A multi-energy community encompassing electrical, gas and heat sub-systems was investigated in [19]. The mixed-integer nonlinear programming (MINLP) formulation accounts for optimal planning and operation of photovoltaic (PV) systems, concluding that combined heat and power units notably contribute to reduce carbon emissions. Ref. [20] deals with optimal day-ahead scheduling of cooperative ECs. In such framework, prosumers interact by sharing surplus PV generation. To this end, the authors proposed a formulation based on alternating direction of multipliers.

Yan et al [21], presented a mixed-integer linear programming (MILP) formulation of optimal day ahead-scheduling of ECs, involving electrical and thermal demands. In that problem, various renewable generators and their corresponding uncertainties are modelled using stochastic programming. A heuristic two-phase (operation-planning) framework was developed in [22], being focused on multi-energy ECs encompassing hybrid storage systems formed by electrical, heat and cool storage systems. The proposed

system includes electric vehicle (EV) loads, which help to reduce energy consumption by 53% when they are provided by the new system.

In net zero ECs, renewable generators play a vital role, but also storage systems, especially battery energy storage (BES) banks. In this regard, Ref. [23] proposes a market mechanism by which prosumers can partake by bidding storage capacity blocks provided by customer-owned BESs. Rao et al [24], developed a grid-friendly energy management strategy for ECs with advanced flexible loads. The aim of this operational strategy is maintaining the stability of the upscale grid, for which the admissible capacity is transferred to local users that run a local market within the considered margins. Despite involving a large variety of unpredictable loads and generators, this model does not contemplate explicit uncertainties modelling.

In [25], the optimal planning of ECs is addressed via MILP formulation. A real case study is concerned for a municipality in Austria, involving six domestic participants. The results reached in this reference demonstrate that energy costs might be reduced by 15% when adopting a community structure in the city. Liu et al [26], designed a deterministic heuristic strategy for ECs involving thermal, ice and electrical storage units, showing that carbon emissions can be reduced by 53% utilizing different storage technologies, when comparing with a benchmark layout with limited storage capacity. In [27], a coordinated day-ahead and intraday scheduling strategy for ECs is developed. The problem formulation is a mixed-integer quadratic programming (MIQP), based on alternating direction of multipliers.

Mustika et al [28], proposed a two-stage approach for optimal operation of ECs. The developed framework decouples the operational phase, from the energy allocation among participants. The authors considered rule-based and MILP optimization-based approaches, in order to evaluate the adequacy of each methodology. The authors of [29]

employed evolutionary algorithms for energy management of ECs. This reference presents a novel community layout, encompassing thermal, cooling and electrical sub-systems, which are co-optimized on a whole. The results presented reveal a clear advantage in jointly considering the different sub-systems, reaching notably cost reductions.

1.3 - Contributions

Literature regarding energy management in ECs has grown notably during the last years; however, this topic is not mature yet and presents various research opportunities. As deduced from Table 1, the related literature is still grey regarding uncertainties modelling in ECs. Moreover, off-grid ECs involving collective assets have been very few studied. This paper aims at filling these gaps, more precisely, the main contributions of this work are as follows:

- Developing a MILP-based day ahead scheduling tool for isolated 100% renewable ECs. The developed mathematical formulation involves individual (rooftop PV units and controllable appliances (CAs)) and collective (BES and wind generators).
- Proposing a three-stage methodology for solution of the contemplated mathematical formulation, by which individual home energy management (HEM) problems are firstly treated, P2P exchanging among prosumers is decided at second stage and collective assets scheduling is solved at third stage.
- Developing a hybrid uncertainties modelling by which stochastic approach is used for considering a variety of wind scenarios, while net demand (to-be-purchased and exportable energy) from prosumers is treated using robust optimization (RO) [30].

As seen in Table 1, this research supposes the first attempt to apply RO in ECs. The novelty and contributions are further incremented by hybridizing this formulation with the conventional stochastic programming. Other merits of the present paper are the consideration of ECs in isolated systems as well as the tractable MILP formulation, which is normally preferred to nonlinear or metaheuristic-based formulations because its low computational burden, global optimum reachability and versatility [20, 25]. A case study is conducted on a variety of scenarios in order to validate the novel proposal as well as analyse the performance of the studied community layout, highlighting the role of individual and collective assets.

Table 1 - A summary of the related literature

Reference	Mathematical modelling	Solver	Uncertainties modelling	Community layout
[19]	MINLP	Analytic	No	• Grid-connected • Multi-energy conversion devices • Multi-energy storage
[20]	MILP	Analytic	No	• Grid-connected • Customer-owned BES • Rooftop PV
[21]	MILP	Analytic	Stochastic	• Grid-connected • Customer-owned BES • Rooftop PV
[22, 26]	MINLP	Heuristic	No	• Grid-connected • Multi-energy storage • PV units
[23, 25]	MILP	Analytic	No	• Grid-connected • Customer-owned BES • Rooftop PV
[24]	MINLP	Metaheuristic	No	• Grid-connected • Customer-owned BES • Rooftop PV
[27]	MIQP	Analytic	Stochastic	• Grid-connected • Customer-owned BES • Rooftop PV
[28]	MILP Rule-based	Analytic	No	• Grid-connected • Customer-owned BES • Rooftop PV
[29]	MINLP	Metaheuristic	No	• Grid connected • Rooftop PV • Hybrid storage system
This paper	MILP	Analytic	Stochastic-RO	• Off-grid • Rooftop PV • Collective BES • Collective wind generators

In the rest of this paper, Section 2 describes the necessary background. Section 3 presents the mathematical formulation of the different stages involved in the new proposal

under deterministic conditions. Section 4 modifies the mathematical notation introduced in Section 3 to contemplate uncertainties via the new stochastic-RO modelling. Section 5 presents a case study with results. The paper is concluded with Section 6.

2 - Background

2.1 - EC layout

This paper focuses on isolated communities, i.e. those that are not connected to an upstream network and, therefore, it must be supplied through its own assets. In consonance with the current legislative framework and available resources in most of rural areas [31, 32], we consider a 100% renewable system for electrical supplying of the community under study. Thereby, renewable generation is responsibility of PV and wind generation units. However, while the former are small-scale customer-owned installations, the wind turbines are collective. This solution is considered more adequate since, while PV panels are currently available at small sizes widely used in domestic installations [33], small-scale wind turbines have not been widely deployed at residential level because their high visual and sound impact [34]. In this regard, we consider that deploying a mid or large-scale wind generation system at collective level is the most viable solution. Likewise, a BES is collectively available.

The community is assumed to be formed by prosumers, which partake in a cooperative way, i.e. without expecting any monetary revenue from their activities [20]. In this way, each prosumer provides generation capacity (through rooftop PV panels) together with demand flexibility enabled by a set of owned CAs (e.g. washing machines, dryers, dishwashers and EVs) [35]. Each prosumer is connected to the community through the proper metering infrastructure, which enables active communication and control from the EC operator, who has the capacity of planning the energy exchanging among prosumers as well as the scheduling plan for the collective assets, as detailed in

the following subsection. For the sake of simplicity, Fig. 1 shows a pictorial representation of the EC under study.

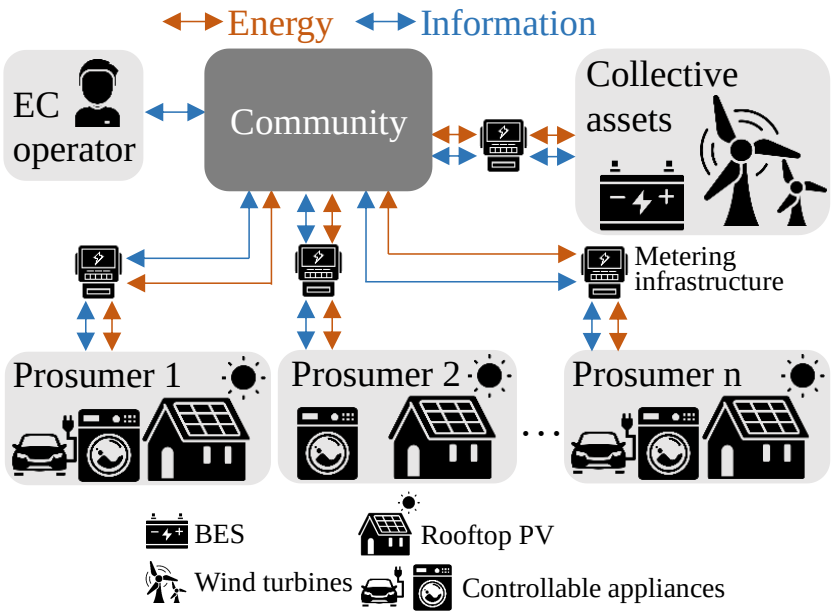

Fig. 1 - Graphical representation of the off-grid EC under study

2.2 - The proposed three-stage scheduling strategy

The operation of the EC described above requires the participation of prosumers and the EC operator, who should interact on pursuing the collective welfare. In this sense, it seems few reasonable trying to operate all the available assets through a conventional single-stage methodology, which may pose intractability and privacy concerns being so few practical [36]. To circumvent this issue, we divide the scheduling mechanism into different sub-problems, from which a three-stage methodology arises as sketched in Fig. 2. The different stages involved are described below:

- **Stage 1**: involves the individual HEM problems for each prosumer in particular, by which the customer-owned assets (i.e. rooftop PV units and CAs) are scheduled with the aim of reducing the energy that must be acquired from the community. In other words, this stage pursues the maximization of the self-consumption of each prosumer individually. This way, the prosumer does not need to interact with any other agent thus avoiding possible privacy issues.

- **Stage 2**: seeks for further maximizing the collective self-consumption through P2P energy exchanging among prosumers. This mechanism enables further exploitation of surplus PV generation that may eventually appear in some prosumers. This excess of energy can be exploited by other prosumers thus reducing the amount of energy that must be acquired from collective assets. This stage is assumed to be performed by the operator, who receives the expected net demand from each prosumer and schedule the energy exchanges.
- **Stage 3**: lastly, the operator decides the scheduling plan for collective assets in order to reduce the non-served energy, thus maximizing the collective welfare. To this end, the community can still take benefit of the non-accommodated exportable energy at stage 2. In this regard, storage facilities play a vital role, allowing a more effective use of the available energy.

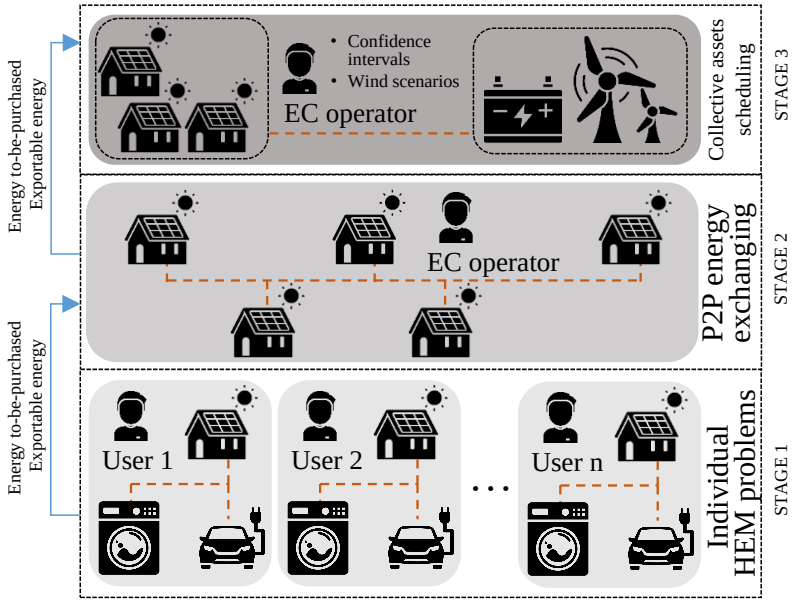

Fig. 2 - Schematic representation of the three-stage scheduling strategy

It is worth noting that Fig. 2 shows that the operator should provide wind scenarios and confidence intervals at stage 3. This information is necessary for hybrid stochastic-RO modelling of uncertainties from wind generation and prosumers' net demand, as detailed in Section 4.

3 - Deterministic mathematical formulation

This section presents the deterministic mathematical formulation of the different stages described in Section 2.2. This formulation is valid for stages 1 and 2, where uncertainties are not contemplated, while Stage 3 is pertinently modified in Section 4 in order to account for uncertainties brought by wind generation and prosumers' net demand.

3.1 - 1st stage: individual HEM problems

At stage 1 the individual HEM problems for each prosumer are performed, which schedule the customer-owned assets with the objective of maximizing the individual self-consumption. The formulation of this sub-problem for the i^{th} prosumer is formulated below. Despite there exist multiple approaches for HEM problems [37, 38], a centralized MILP-based formulation has been used here, which has been widely studied and presents multiple advantages (e.g. see [39, 40]).

Since each peer aims at maximizing the collective welfare, the objective of each prosumer will be minimizing his importable energy, as follows:

$$\mathrm{E}\left(p_{i|t}^{pur}\right), \mathrm{E}\left(p_{i|t}^{\exp}\right) \leftarrow \min_{\Psi^{HEM}} \Delta\tau \cdot \left\{p_{i|t}^{pur}\right\}; \forall i \in Q \tag{1}$$

where Ψ^{HEM} is the vector of decision variables of the 1st stage, which is given by

$$\Psi^{HEM} = \left\{ \begin{array}{c} p_{i|t}^{pur}, p_{i|t}^{exp}, p_{i|t}^{PV}, \pi_{i|t}^{a}, \\ \pi_{i|t}^{pur}, \pi_{i|t}^{exp}, \mathrm{on}_{i|t}^{aa}, \mathrm{off}_{i|t}^{aa}, \\ p_{i|t}^{HVAC,x}, p_{i|t}^{EWH}, \theta_{i|t}^{air,in}, \theta_{i|t}^{W,h} \end{array} \right\}; \begin{array}{c} \forall i \in Q \wedge \forall t \in T \wedge \forall a \in A_{NI}^{i} \cup A_{I}^{i} \\ \wedge \forall aa \in A_{NI}^{i} \wedge x = h \vee c \end{array} \tag{2}$$

The 1st stage of the developed optimization framework is subjected to multiple constraints, which are detailed in subsequent sections.

Home balance

The home power balance is established in (3), while (4) and (5) avoid simultaneous imports and exports [20].

$$p_{i|t}^{pur} + p_{i|t}^{PV} = p_{i|t}^{exp} + p_{i|t}^{NC} + \sum_{a \in A^i} \left\{ \pi_{i|t}^{a} \cdot p^{a} \right\}; \forall i \in Q \wedge t \in T \quad (3)$$

$$p_{i|t}^{k} \leq \pi_{i|t}^{k} \cdot \overline{p}_i; \forall i \in Q \wedge t \in T \wedge k = pur \vee exp \quad (4)$$

$$\pi_{i|t}^{pur} + \pi_{i|t}^{exp} \leq 1; \forall i \in Q \wedge t \in T \quad (5)$$

PV modelling

The PV potential as a function of solar irradiance and ambient temperature is calculated by (6) [41], which is complemented by (7), thus avoiding unrealistic PV generation [42].

$$\phi_{i|t}^{PV} = \overline{p}_i^{PV} \cdot \left[0.25 \cdot \vartheta_t + 0.03 \cdot \vartheta_t \cdot \theta_t^{air,out} + \left(1.01 + 1.13 \cdot \frac{\eta_i^{PV}}{100} \right) \cdot \vartheta_t^2 \right]; \forall i \in Q \wedge t \in T \quad (6)$$

$$p_{i|t}^{PV} \leq \begin{cases} \phi_{i|t}^{PV}, \text{if } \phi_{i|t}^{PV} \leq \overline{p}_i^{PV} \\ \overline{p}_i^{PV}, \text{o.w.} \end{cases}; \forall i \in Q \wedge t \in T \quad (7)$$

Controllable appliances

CAs are divided into interruptible and non-interruptible. The formers can interrupt their operation in contrast to the latter [42]. The constraint (8) ensures that each controllable appliance completes its duty cycle within predefined time windows, while (9) and (10) impose continuity in the operation of non-interruptible appliances [42].

$$\sum_{t \in \Theta_i^a} \left\{ \pi_{i|t}^{a} \right\} = \frac{\delta_a}{\Delta \tau}; \forall i \in Q \wedge a \in A_{NI}^i \cup A_I^i \quad (8)$$

$$\pi_{i|t}^{a} - \pi_{i|t-1}^{a} = \text{on}_{i|t}^{a} - \text{off}_{i|t}^{a}; \forall i \in Q \wedge t \in T \setminus t > 1 \wedge a \in A_{NI}^i \quad (9)$$

$$\sum_{t \in \Theta_i^a} \left\{ \text{on}_{i|t}^{a} \right\} = 1; \forall i \in Q \wedge a \in A_{NI}^i \quad (10)$$

Heating-ventilation-air conditioner (HVAC) modelling

The linear variation of indoor temperature as a function of outdoor temperature and the action of the HVAC system is established in (11) [43]. It is realistic to assume that

HVAC systems cannot be operated in heating and cooling modes simultaneously, as said (12), whereas (13) limits the consumption of HVAC devices to rated values. The constraint (14) ensures that indoor temperature is kept within comfortable bounds, while (15) equals the initial and final indoor temperatures to set-point settings, as customary [42].

$$\theta_{i|t}^{air,in} = \left(1 - \frac{\Delta\tau}{10^3 \cdot m_i^{air,in} \cdot C^{air} \cdot R_i^{build}}\right) \cdot \theta_{i|t-1}^{air,in} + \frac{\Delta\tau}{10^3 \cdot m_i^{air,in} \cdot C^{air} \cdot R_i^{build}} \cdot \theta_{i|t-1}^{air,out} + \frac{\Delta\tau \cdot \left(p_{i|t}^{HVAC,h} - p_{i|t}^{HVAC,c}\right)}{0.000277 \cdot m_i^{air,in} \cdot C^{air}} \cdot COP_i^{HVAC}; \forall i \in Q \wedge t \in T \setminus t > 1 \quad (11)$$

$$\pi_{i|t}^{HVAC,h} + \pi_{i|t}^{HVAC,c} \leq 1; \forall i \in Q \wedge t \in T \quad (12)$$

$$p_{i|t}^{HVAC,k} \leq \pi_{i|t}^{HVAC,k} \cdot \overline{p}_i^{HVAC}; \forall i \in Q \wedge t \in T \wedge k = h \vee c \quad (13)$$

$$\theta_i^{HVAC,sp} - \theta_i^{HVAC,db} \leq \theta_{i|t}^{air,in} \leq \theta_i^{HVAC,sp} + \theta_i^{HVAC,db}; \forall i \in Q \wedge t \in T \quad (14)$$

$$\theta_{i|T(1)}^{air,in} = \theta_{i|T(\text{end})}^{air,in} = \theta_i^{HVAC,sp}; \forall i \in Q \quad (15)$$

Electric water heater (EWH) modelling

The model established by (16) and (17) yields the hot water temperature depending on the instantaneous water consumption [43], while (18)-(20) are analogue to (13)-(15) but particularized to EWHs.

$$\theta_{i|t+1}^{w,h} = \theta_{i|t}^{w,h} + p_{i|t}^{EWH} \cdot \eta_i^{EWH} \cdot C^{w,h} - \left(\theta_{i|t}^{air,in} - \theta_{i|t}^{w,h}\right) \cdot e^{\frac{\Delta\tau}{R^{w,h} \cdot C^{w,h}}}; \forall i \in Q \wedge t \in T \setminus t < \text{size}(T) \wedge v_{i|t}^{w,h} = 0 \quad (16)$$

$$\theta_{i|t+1}^{w,h} = \frac{\theta_{i|t}^{w,h} \cdot \left(\overline{v}_i^{EWH} - v_{i|t}^{w,h}\right) + \theta_{i|t}^{w,c} \cdot v_{i|t}^{w,h}}{\overline{v}_i^{EWH}}; \forall i \in Q \wedge t \in T \setminus t < \text{size}(T) \wedge v_{i|t}^{w,h} > 0 \quad (17)$$

$$p_{i|t}^{EWH} \leq \overline{p}_i^{EWH}; \forall i \in Q \wedge t \in T \quad (18)$$

$$\theta_i^{EWH,sp} \leq \theta_{i|t}^{w,h} \leq \overline{\theta}_i^{EWH}; \forall i \in Q \wedge t \in T \quad (19)$$

$$\theta_{i|T(1)}^{w,h} = \theta_{i|T(\text{end})}^{w,h} = \theta_i^{EWH,sp}; \forall i \in Q \tag{20}$$

It is worth noting that the model above does not contemplate individual BES. This is due to the considered EC counts with a collective BES from which all the prosumers can be benefited. In this regard, it is assumed that individual BESs are not attractive or even can be conflictive with the interests of the community. For example, a prosumer could store energy in order to speculate and send it back to the grid against the collective welfare. In this sense, we consider that a collective storage system is more practical and fairer in cooperative communities. Nevertheless, this kind of systems can be easily incorporated into the model as well as electric vehicles following the formulations in [39, 40], or even these devices can be considered collective assets as in [23].

3.2 - 2nd stage: energy exchanges among prosumers

This stage enables energy exchanges among prosumers, with the objective of further reducing the net demand from residential users. To this end, some users who present low self-generation or high demand can exploit surplus PV generation from others. Therefore, the objective of this stage is reducing the energy that must be purchased from collective assets. This parameter can be easily calculated by accumulating the importable power of all the prosumers involved as in (21), which allows to formulate the objective function of the 2nd stage (22).

$$ECB = \Delta\tau \cdot \sum_{\forall t \in T} \left\{ \sum_{\forall i \in Q} \left\{ p_{i|t}^{pur} \right\} \right\} \tag{21}$$

$$\mathrm{E}\left(p_{i|t}^{EC,pur} \right), \mathrm{E}\left(p_{i|t}^{EC,\exp} \right) \leftarrow \min_{\Psi^{P2P}} ECB\left(\mathrm{E}\left(p_{i|t}^{pur} \right), \mathrm{E}\left(p_{i|t}^{\exp} \right) \right); \forall i \in Q \tag{22}$$

where Ψ^{P2P} is the vector of decision variables of the 2nd stage given by

$$\Psi^{P2P} = \left\{ p_{i\to j|t}, p_{j\to i|t}, p_{i|t}^{EC,pur}, p_{i|t}^{EC,exp} \right\}; \forall i, j \in Q \wedge t \in T \tag{23}$$

As expressed in (22), this stage calculates the expected energy that must be acquired from collective assets at stage 3. Likewise, eventual exportable power is also calculated, which is sent to the 3rd stage to be leveraged by collective BESs. Different constraints must be imposed at this stage in order to properly model the energy exchanges among prosumers. Firstly, (24) indicates that a prosumer cannot exchange more power than the expected surplus PV generation.

$$\sum_{\substack{\forall j \in Q \\ j \neq i}} \left\{ p_{i \to j|t} \right\} \leq p_{i|t}^{exp}; \forall i \in Q \wedge t \in T \tag{24}$$

In (24), the left-hand side indicate the power exported by the i^{th} prosumer and imported by the j^{th} prosumer. The power balance (25) stands for the generation-consumption balance accounting for energy exchanges among prosumers.

$$p_{i|t}^{pur} + p_{i|t}^{EC,exp} + \sum_{\substack{\forall j \in Q \\ j \neq i}} \left\{ p_{i \to j|t} \right\} = p_{i|t}^{exp} + p_{i|t}^{EC,pur} + \sum_{\substack{\forall j \in Q \\ j \neq i}} \left\{ p_{j \to i|t} \right\}; \forall i \in Q \wedge t \in T \tag{25}$$

In contrast to (3), the balance (25) only includes transactions among prosumers and collective assets, neglecting the scheduling of prosumer-owned devices such as PV panels or CAs. Finally, the constraint (26) establishes individual balance for each ij^{th} pair of prosumers [20].

$$p_{i \to j|t} = p_{j \to i|t}; \forall i, j \in Q \wedge t \in T \tag{26}$$

3.3 - 3rd stage: collective assets scheduling

Finally, the operator decides the scheduling plan for the collective assets (wind generator and BES) in order to satisfy as much demand as possible. To this end, the operator receives the resulting net demand from the second stage and, on the basis of this information, establishes the power allocation among collective units. The objective of this stage is minimizing the operational cost including compensatory payments for non-served energy, as follows

$$\min_{\Psi^{EC}} Cost = \Delta\tau \cdot \sum_{\forall t \in T} \left\{ \lambda^{NS} \cdot p_t^{NS} + \mu^{WG} \cdot p_t^{WG} + \mu^{BES} \cdot \left(p_t^{BES,ch^2} + p_t^{BES,dch^2} \right) \right\} \quad (27)$$

where Ψ^{EC} is the vector of decision variables of the 3rd stage given by

$$\Psi^{EC} = \left\{ \begin{matrix} p_t^{BES,k}, \pi_t^{BES,k}, \\ p_t^{NS}, p_t^{WG}, \varepsilon_t^{BES} \end{matrix} \right\}; \forall t \in T \wedge k = ch \vee dch \quad (28)$$

The objective function (27) stands for the operational cost, which includes the cost of non-served energy together with operational and maintenance expenditures of wind turbines and batteries. In this case, operational and maintenance costs of BESs have been considered a quadratic function of the energy exchanged with the grid [44]. To preserve the MILP structure of the formulation, the quadratic terms in (27) are linearized using piecewise representations [45].

Together with the objective function (27), this stage includes a series of constraints as explained below. Firstly, (29) is the power balance of the community accounting for wind generators and collective storage assets.

$$p_t^{BES,dch} + p_t^{WG} + p_t^{NS} + \sum_{\forall i \in Q} \left\{ \mathbb{E}\left(p_{i|t}^{EC,\exp} \right) \right\} = p_t^{BES,ch} + \sum_{\forall i \in Q} \left\{ \mathbb{E}\left(p_{i|t}^{EC,pur} \right) \right\}; \forall t \in T \quad (29)$$

The model (30) represents the wind power potential according to the well-known wind-power curve of wind turbines [46, 47]. In this expression, $\gamma^{WG,*}$ is the rated speed of wind turbines, which stands for that speed value for which the turbine yields its rated power $\overline{p}^{WG}$.

$$\frac{\eta^{WG}}{100} \cdot p_t^{WG} \leq \begin{cases} 0, \text{if } \gamma_t \leq \underline{\gamma}^{WG} \text{ or } \gamma_t \geq \overline{\gamma}^{WG} \\ \alpha \cdot \gamma_t^3 - \beta \cdot \overline{p}^{WG}, \text{if } \underline{\gamma}^{WG} \leq \gamma_t \leq \gamma^{WG,*}; \forall t \in T \\ \overline{p}^{WG}, \text{if } \gamma^{WG,*} \leq \gamma_t \leq \overline{\gamma}^{WG} \end{cases} \quad (30)$$

It is assumed that the community counts with a collective storage system formed by batteries since this technology is, by far, the most widely used in isolated microgrids [48, 49]. In this case, the maximum power that can be exchanged by BES is given by its

nominal capacity and the energy-to-power ratio [50], as said (31), whereas (32) avoids simultaneous charging-discharging of the battery bank. The model (33) expresses the dynamics of the batteries [51] and (34) limits the energy stored to the nominal capacity and depth-of-discharge settings. Finally, the model is completed with (35), which establishes coherency in the battery cycle over the considered time horizon [52].

$$p_t^{BES,k} \le \pi_t^{BES,k} \cdot \frac{\bar{\varepsilon}^{BES}}{\mathrm{e2P}}; \forall t \in T \wedge k = ch \vee dch \tag{31}$$

$$\pi_t^{BES,ch} + \pi_t^{BES,dch} \le 1; \forall t \in T \tag{32}$$

$$\varepsilon_t^{BES} = \varepsilon_{t-1}^{BES} + \Delta\tau \cdot \left(\frac{\eta^{BES} \cdot p_t^{BES,ch}}{100} - \frac{100 \cdot p_t^{BES,dch}}{\eta^{BES}} \right); \forall t \in T \setminus t > 1 \tag{33}$$

$$\left(1 - \frac{\mathrm{DOD}}{100}\right) \cdot \bar{\varepsilon}^{BES} \le \varepsilon_t^{BES} \le \bar{\varepsilon}^{BES}; \forall t \in T \tag{34}$$

$$\varepsilon_{T(1)}^{BES} = \varepsilon_{T(\mathrm{end})}^{BES} = \bar{\varepsilon}^{BES} \tag{35}$$

It is worth commenting that network modelling has not been included in the model above. This is due to ECs are normally small-scale networks where prosumers are located close to each other. Under these assumptions, the effect of grid parameters is negligible [53], and phenomena like dynamic thermal rating [54, 55] can be ignored.

4 - The developed stochastic-RO for uncertainties modelling

4.1 - Foundations

For optimal day-ahead scheduling of the EC described in Section 2, the operator should be aware of various uncertainties. In this case, prosumers' net demand and wind speed are essentially uncertain parameters. However, these both uncertainties may present different character and features. Thus, while net demand can be predicted with certain accuracy due to it is subjected to foreseeable weather parameters and human routines, wind speed may randomly vary over the considered time horizon [56]. By these reasons,

we develop a hybrid stochastic-RO approach for uncertainties modelling, by which wind speed is modelled via scenarios while net demand is treated using RO subjected to confidence intervals imposed by the operator. It is worth mentioning that similar approaches have been used in other optimization problems [57], showing good results.

4.2 - Stochastic programming

Stochastic programming is statistical-based methodology that has been widely employed for modelling of uncertainties, which can be represented by probability distributions or historical data [58, 59]. Basically, this approach consists on generating a large number of scenarios (normally ~1000 [60]) for the concerned unknown. Then, the problem is solved as many times as scenarios are considered, obtaining statistical information of the outputs following the distribution of inputs.

Frequently, the number of scenarios to be generated entails intractability problems. To solve this issue, data reduction techniques have been extensively employed [61]. These techniques reduce a set of data to a minimum group of representative profiles. Among the different data reduction approaches available, clustering methods are frequently employed because their simplicity and easy codification [62]. In this paper, the k-medoids method is considered due to its good overall features [63]. This technique collects the original data into clusters, which are represented by only a member called medoid. Thereby, the original scenario-space can be reduced to a reduced set of representative profiles. To determine the optimal number of clusters (i.e. representative scenarios), heuristic indexes are normally considered [16]. These indexes look for the minimum number of scenarios for which acceptable accuracy is achieved, thus resulting in an optimal trade-off between reliability and efficiency. Once the representative set has been constructed, the probability of each representative scenario can be calculated by

$$\omega_r = \frac{\text{size}\left(\Omega_r\right)}{\text{size}\left(S\right)}; \forall r \in R \tag{36}$$

4.3 - Robust reformulation of optimization problems

Unlike stochastic programming, RO is a non-statistical methodology for uncertainties modelling, which is based on representing an unknown by its expected profile and its associated confidence intervals (represented by the Δ's), as sketched Fig. 3. This way, the generic uncertain *w* can be represented as an interval number [64], as follows:

$$w_{mn} \in \left[\mathbb{E}\left(w_{mn}\right) - \Delta w_{mn}, \mathbb{E}\left(w_{mn}\right) + \Delta w_{mn}\right]; \forall m, n \in J_m \tag{37}$$

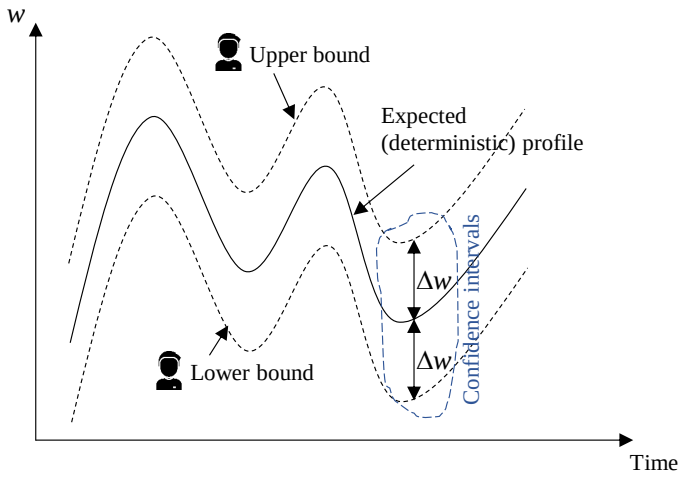

Fig. 3 - Sketch of the interval representation considered in this paper for RO

where J_m is the subset of uncertain parameters. According to (37), RO reformulates a generic minimization problem including a max sub-problem that aims at maximizing the deviation of uncertainties, as follows (see [65] for further details):

$$\min_{\boldsymbol{\Xi}} \boldsymbol{c}^{\mathrm{T}} \cdot \boldsymbol{\Xi} \tag{38}$$

Subject to:

$$\begin{aligned} &\sum_{\forall n} \left\{ w_{mn} \cdot \xi_m \right\} + \max_{\left\{ L_m \cup \{h_m\} \middle| L_m \subseteq J_m, |L_m| \le \Gamma_m, h_m \in J_m \setminus L_i \right\}} \\ &\sum_{\forall n \in L_0} \left\{ \Delta w_{mn} \cdot \left|\xi_n\right| + \left(\Gamma_m - \left\lfloor \Gamma_m \right\rfloor\right) \cdot \Delta w_{mn} \cdot \left|\xi_{h_m}\right| \right\} \le b_m; \forall m \end{aligned} \tag{39}$$

$$\begin{cases} \underline{\boldsymbol{\Xi}} \le \boldsymbol{\Xi} \le \overline{\boldsymbol{\Xi}} \\ \xi_m; \forall m \in \{1, 2, ..., M\} \end{cases} \tag{40}$$

where $\boldsymbol{c}$ is the vector of costs, $\xi_m \in \boldsymbol{\Xi}$ are the decision variables of the deterministic model, $b_m \in \boldsymbol{b}$ is the vector of inequality constraints and $\Gamma \in \mathbb{R}^+$ is the so-called robust parameter, which sets the degree in which the confidence intervals are considered (the whole interval is considered for $\Gamma = 1$ while the problem becomes deterministic if $\Gamma = 0$). The optimization problem above cannot be solved by conventional methods because the nested min-max problem in (39). To circumvent this barrier, an alternative formulation was proposed in [66], which is based on the strong duality theorem. Thereby, the problem (38)-(40) can be reduced to a simpler minimization framework, as follows:

$$\min_{\boldsymbol{\Xi},\boldsymbol{z},\boldsymbol{q},\boldsymbol{y}} \boldsymbol{c}^{\mathrm{T}} \cdot \boldsymbol{\Xi} \tag{41}$$

Subject to:

$$\begin{cases} \sum_{\forall n} \left\{ w_{mn} \cdot \xi_j \right\} + z_m \cdot \Gamma_m + \sum_{n \in J_i} \left\{ q_{mn} \right\} \le b_m ; \forall m \\ z_m + q_{mn} \ge \Delta w_{mn} \cdot y_n ; \qquad \forall m \ne 0 \wedge n \in J_0 \\ q_{mn}, z_m, y_n \ge 0; \qquad \forall m, n \in J_m \\ -y_n \le \xi_n \le y_n ; \qquad \forall n \\ \underline{\boldsymbol{\Xi}} \le \boldsymbol{\Xi} \le \overline{\boldsymbol{\Xi}} \\ \xi_m ; \qquad \forall m \in \{1, 2, ..., M\} \end{cases} \tag{42}$$

where $\boldsymbol{z}$, $\boldsymbol{q}$ and $\boldsymbol{y}$ are the vectors which collect the set of variables z's, q's and y's, respectively. These variables are introduced to linearize the original problem (38)-(40), and enlarge the decision space as seen in (41). It is worth noting that, unlike to the formulation proposed in [66], we assume that the vector $\boldsymbol{c}$ is perfectly known.

4.4 - The modified 3rd stage considering Stochastic-RO formulation

To accommodate the hybrid stochastic-RO model described in previous sections, problem (25)-(32) has to be rewritten following the framework (41) and (42). Moreover, the wind speed scenarios have to be considered according their probability of occurrence. Thus, the original objective function (27) is replaced by (43).

$$\min_{\Psi^{EC}} Cost = \sum_{r\in R}\left\{\frac{\omega_r}{100}\cdot\sum_{t\in T}\left\{\Delta\tau\cdot\left[\lambda^{NS}\cdot p_t^{NS}+\mu^{WG}\cdot p_t^{WG}+\mu^{BES}\cdot\left(p_t^{BES,ch^2}+p_t^{BES,dch^2}\right)\right]\right\}\right\} \tag{43}$$

where Ψ^{EC-RO} is the vector of decision variables for the modified 3rd stage, as follows

$$\Psi^{EC-RO}=\left\{\begin{matrix} p_{r|t}^{BES,k}, \pi_t^{BES,k}, z_{r|t}^{Balance}, q_{r|t}^{Balance,x}, \\ y_t^{Balance,x}, p_{r|t}^{NS}, p_{r|t}^{WG}, \varepsilon_{r|t}^{BES} \end{matrix}\right\}; \quad \forall t\in T\wedge k=ch\vee dch\wedge x=EC,pur\vee EC,exp \tag{44}$$

As seen, the vector (44) is basically an extended version of (27) to incorporate the z 's, q 's and y 's. These dummy variables will appear wherever the prosumers' net demand is included since, as discussed previously, this uncertainty is modelled using RO. On the other hand, wind speed is modelled using scenarios, which leads to extend the variable space including the number of representative scenarios (i.e. the space R). This is the reason why some variables incorporate the index r together with the time. The probability of each scenario is also taken into account in (43).

Therefore, the constraints (29)-(35) must be modified according the novel framework. Firstly, the power balance (29) is replaced by

$$\sum_{\forall i\in Q}\left\{\mathbb{E}\left(p_{i|t}^{EC,pur}\right)-\mathbb{E}\left(p_{i|t}^{EC,\exp}\right)\right\}-p_{r|t}^{BES,dch}-p_{r|t}^{WG}-p_{r|t}^{NS}+p_{r|t}^{BES,ch}+z_{r|t}^{Balance}\cdot\Gamma+q_{r|t}^{Balance,EC,pur}+q_{r|t}^{Balance,EC,exp};\forall r\in R\wedge t\in T \tag{45}$$

As observed, the equation (45) is basically equal to (29) but according to the robust formulation depicted in (42). In (45), the variables present two indexes. One for the time, and another for the representative scenario. In this way, the expression (29) is modified to incorporate the proposed stochastic-RO formulation. According to (42), the expression (45) needs to impose the additional constraints (46)-(48), to properly model the confidence intervals associated to the prosumers' net demand.

$$z_{r|t}^{Balance}+q_{r|t}^{Balance,x}\geq y_t^x\cdot\Delta p_t^x;\forall r\in R\wedge t\in T\wedge x=EC,pur\vee EC,exp \tag{46}$$

$$1 \le y_t^x; \forall t \in T \wedge x = EC, pur \vee EC, exp \tag{47}$$

$$z_{r|t}^{Balance}, q_{r|t}^{Balance,x}, y_t^x \ge 0; \forall r \in R \wedge t \in T \wedge x = EC, pur \vee EC, exp \tag{48}$$

The remainder constraints can be easily modified by extending the variable-space to accommodate the representative scenarios, since they are not influenced by the prosumers' net demand, (30)-(35) are replaced by (49)-(54), respectively.

$$\frac{\eta^{WG}}{100} \cdot p_{r|t}^{WG} \le \begin{cases} 0, \text{if } \gamma_{r|t} \le \underline{\gamma}^{WG} \text{ or } \gamma_{r|t} \ge \overline{\gamma}^{WG} \\ \alpha \cdot \gamma_{r|t}^3 - \beta \cdot \overline{p}^{WG}, \text{if } \underline{\gamma}^{WG} \le \gamma_{r|t} \le \gamma^{WG,*}; \forall r \in R \wedge t \in T \\ \overline{p}^{WG}, \text{if } \gamma^{WG,*} \le \gamma_{r|t} \le \overline{\gamma}^{WG} \end{cases} \tag{49}$$

$$p_{r|t}^{BES,k} \le \pi_t^{BES,k} \cdot \frac{\overline{\varepsilon}^{BES}}{\mathrm{e2P}}; \forall r \in R \wedge t \in T \wedge k = ch \vee dch \tag{50}$$

$$\pi_t^{BES,ch} + \pi_t^{BES,dch} \le 1; \forall t \in T \tag{51}$$

$$\varepsilon_{r|t}^{BES} = \varepsilon_{r|t-1}^{BES} + \Delta\tau \cdot \left(\frac{\eta^{BES} \cdot p_{r|t}^{BES,ch}}{100} - \frac{100 \cdot p_{r|t}^{BES,dch}}{\eta^{BES}} \right); \forall r \in R \wedge t \in T \setminus t > 1 \tag{52}$$

$$\left(1 - \frac{\mathrm{DOD}}{100}\right) \cdot \overline{\varepsilon}^{BES} \le \varepsilon_{r|t}^{BES} \le \overline{\varepsilon}^{BES}; \forall r \in R \wedge t \in T \tag{53}$$

$$\varepsilon_{r|T(1)}^{BES} = \varepsilon_{r|T(\mathrm{end})}^{BES} = \overline{\varepsilon}^{BES}; \forall r \in R \tag{54}$$

5 - Case study

This section presents a case study with results. The developed mathematical formulation was coded under Matlab R2020a and the resulting optimization problems were solved using Gurobi [67]. All the simulations were run on an Intel® Core™ i5-9400 F, 2.90 GHz, 8.00 GB RAM, over a 24-h horizon. The time step is fixed equal to 30-min, although its influence on the computational performance of the developed framework is studied specifically.

5.1 - Data

A six-prosumer EC is considered for illustrative purposes. Each prosumer can exchange up to 10 kW with others. Fig. 4 plots the expected solar irradiance and ambient temperature together with the representative scenarios for wind speed, which correspond to real data observed at Virgin Islands in 2019 [68]. The wind speed scenarios have been generated following the procedure described in Section 4.2. To determine the optimal number of scenarios to be considered, we compared the total sum of distances and the Davies Bouldin index, which are two widely used indicators [16], thus reducing the yearly data in [68] to only 15 representative profiles that can be managed by average computers. All the prosumers are assumed to be geographically close each other, so that the weather parameters plotted in Fig. 4 affects to the whole community. On the other hand, Fig. 5 shows the expected non-controllable demand and hot water consumption of each prosumer. While, the non-controllable demand has been constructed on the basis of the data in [33, 69], the expected hot water consumption has been taken from [70].

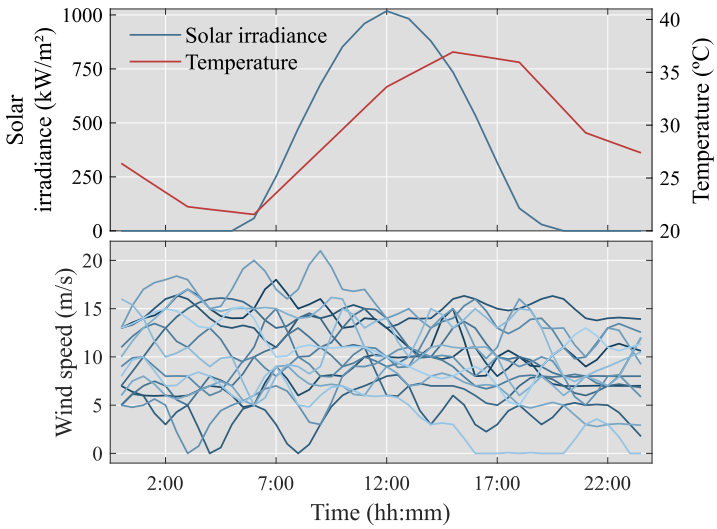

Fig. 4 - Expected solar irradiance, temperature and wind speed scenarios used in simulations

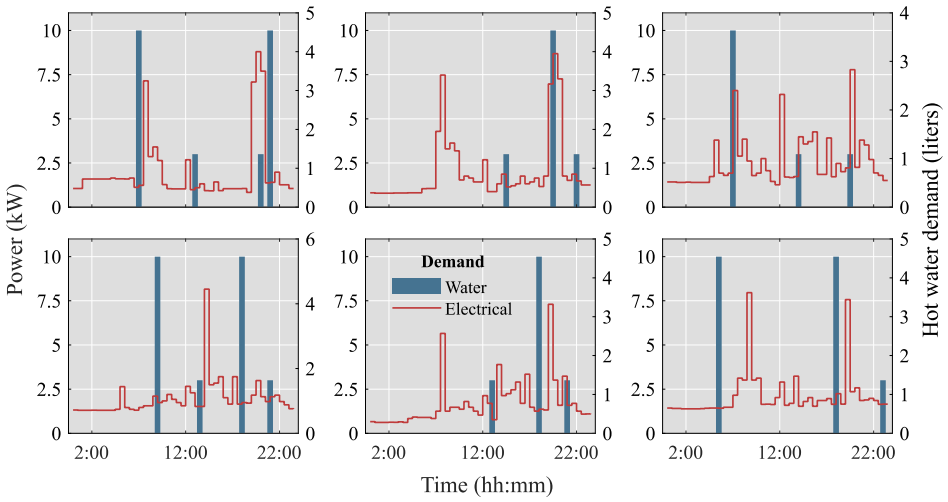

Fig. 5 - Expected prosumers' demand

The ambient parameters reported in Fig. 4 allow to calculate the expected PV potential of each prosumer. Individual rooftop panels are installed in each household with peak power and efficiency reported in Table 2 [70]. Each prosumer installs a set of CAs together with thermostatically controlled devices (HVAC and EWH), whose relevant data is reported in Tables 3-5 based on the parameters described in [33]. A collective Li-ion battery pack has been considered with 98% charging-discharging efficiency and 2 hours energy-to-power ratio [50]. The storage capacity has been fixed in 50 kWh according to the characteristics of prosumers, setting the depth-of-discharge in 60%, as recommended some references to avoid a fast degradation of batteries [16]. A group of wind turbines with 25 kW total installed capacity has been considered, assuming 2, 11 and 21 m/s as cut-on, nominal and cut-off nominal speeds. The efficiency of turbine machinery and electronic devices is considered equal to 85%, while the other parameters related to the wind-power curve are taken equal to [16]. Finally, a degradation cost of 10^{-6} \$/kWh^2 and 0.24 \$/kWh has been considered for batteries and wind turbines, respectively [16, 44]. Finally, 20% confidence intervals are considered for RO modelling.

Table 2 - PV data

Prosumer #	$\overline{p}_i^{PV}$	η_i^{PV}
1	2 kW	16.7%
2	1.5 kW	
3	2 kW	
4	1.2 kW	
5	2 kW	
6	1.5 kW	

Table 3 - CAs data

Prosumer #	δ^a	p^a	Time window	Type
1	3 h	3 kW	8:00-12:00 h	Interruptible
2	2.5 h	2.75 kW	7:00-16:00 h	Interruptible
	1 h	2.5 kW	16:30-21:00 h	Non-interruptible
3	2 h	2.5 kW	18:00-21:00 h	Non-interruptible
4	3 h	3 kW	3:00-7:30 h	Interruptible
	2 h	2 kW	11:00-17:00 h	Non-interruptible
5	3 h	3 kW	10:00-20:00 h	Interruptible
6	3 h	3 kW	0:00-9:00 h	Interruptible
	1.5 h	2.5 kW	10:00-13:00 h	Non-interruptible

Table 4 - HVAC data

Prosumer #	$m_i^{air,in}$	C^{air}	R_i^{build}	COP_i^{HVAC}	$\overline{p}_i^{HVAC}$	$\theta_i^{HVAC,sp}$	$\theta_i^{HVAC,db}$
1	1,778 kg	1.01 kJ/(kg·ºC)	3.2x10^{-6} kW/ºC	1.20	2 kW	23 ºC	0.5 ºC
2	2,223 kg				2 kW	23 ºC	0.5 ºC
3	2,667 kg				2.2 kW	25 ºC	1 ºC
4	1,185 kg				1.8 kW	22 ºC	0.3 ºC
5	2,371 kg				2.1 kW	23 ºC	0.5 ºC
6	2,276 kg				2 kW	24 ºC	0.5 ºC

Table 5 - EWH data

Prosumer #	η_i^{EWH}	$C^{W,h}$	$R^{W,h}$	$\theta_{i\|t}^{W,c}$	$\overline{p}_i^{EWH}$	$\theta_i^{EWH,sp}$	$\overline{\theta}_i^{EWH}$	$\overline{v}_i^{EWH}$
1	90%	1.52 ºC/kW	863.4 ºC/kWh	10 ºC	2 kW	45 ºC	60 ºC	50 gal
2					2.1 kW	40 ºC		45 gal
3					1.8 kW	40 ºC		55 gal
4					2 kW	45 ºC		60 gal
5					2.1 kW	40 ºC		40 gal
6					1.5 kW	45 ºC		50 gal

5.2 - Validation and results analysis

Firstly, we aim at validating the new proposal. To this end, the original settings are preserved as described at the beginning of Section 5. During stages 1 and 2 of the developed methodology deterministic conditions are assumed. The first stage is performed individually by each user, optimally scheduling its own assets in order to reduce the energy that must be purchased from the community. Fig. 6 plots the result

example for the prosumer 6. This household installation accounts for two CAs. One of them must be scheduled during noon before 9:00 h (e.g. an EV). Under these circumstances, the HEM module decided to schedule this appliance at early morning, when the PV generation starts to increase. For the other CA, it is scheduled during time slots with the highest PV generation. Following this principle, a considerable portion of the home demand can be covered by on-site PV generation, without recurring to other collective assets.

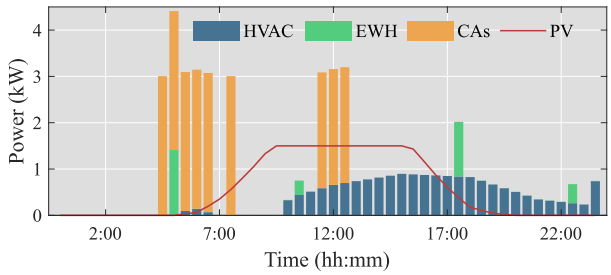

Fig. 6 - HEM result for the prosumer 6

After running each HEM problem individually, the resulting to-be-purchased and exportable energies are calculated. These values are sent to the operator, who performs the stage 2 of the developed procedure when P2P energy exchanges are enabled. At this step, prosumers can exchange energy in order to further reduce their demand, thus reducing the necessity of acquiring energy from collective assets. Fig. 7 plots the importable power profile before and after running the P2P process. As observed, stage 2 allows to reduce the energy that must be purchased from collective storage and generation assets. In fact, total energy is reduced by 1.2 kWh. P2P process is especially notable during the central hours of the day, when PV penetration is still high. During those time slots, eventual surplus PV generation from some prosumers can be exploited by others, thus further reducing the amount of energy that must be accommodated at stage 3.

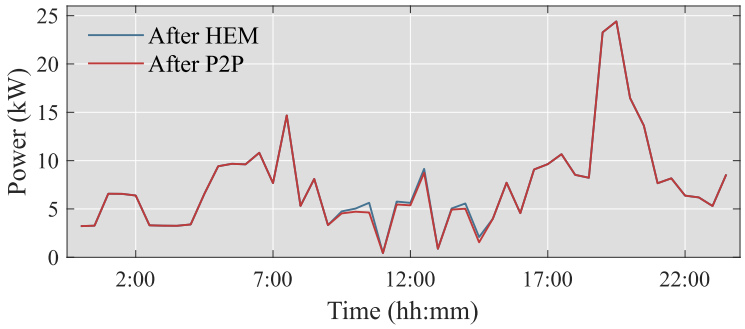

Fig. 7 - To-be-purchased power before and after running the P2P process

At stage 3, uncertainty from wind speed and prosumers' net demand is considered using the models described throughout this paper. For further analysing the role of collective assets in isolated ECs, two scenarios are studied namely 'wind' and 'wind + BES'. In the first case, only wind turbines are deployed without storage capacity. In the face of this situation, wind energy can be only exploited when it is actual generated. In contrast, a battery bank is deployed in the second case, allowing a more efficient use of renewable energy. Fig. 8 analyses the impact of the robust parameter (Γ) on the objective function (operating cost). This parameter sets the degree of robustness of the problem, so that the higher value of Γ, the more uncertainty aware the scheduling mechanism is. It is clearly observed in Fig. 8, where the objective function increases with the value of the robust parameter. As expected, the operating cost was always higher in case of only deploying wind generators without batteries (+13-19%). The objective function is approximately incremented by 37% as the robust parameter grows, from which one can deduce that the cost of robustness is equal to 68 $ in this case. It means that the operator can increment the level of robustness of the scheduling plan but only at expenses of his monetary incomes.

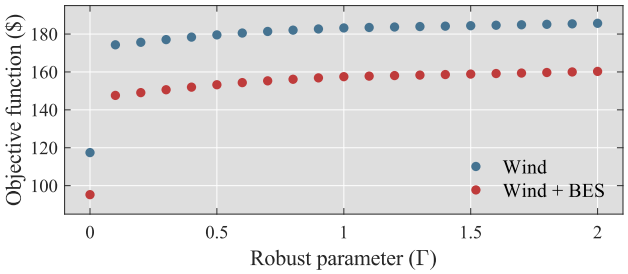

Fig. 8 - Total operating cost for various values of the robust parameter

The increment on the operating cost observed in Fig. 8 is due to the expected prosumers' net demand is incremented with the value of the robust parameter, in order to account for the inherent uncertainty of this parameter. Consequently, the operator assumes unfavourable profiles for the exportable and to-be-purchased energies drawn from stage 2, as seen in Fig. 9. This figure is complemented with Fig. 10, where the evolution of uncertainties with Γ is plotted, observing variations of 28% and 40% in the importable and exportable total energies, respectively. As seen, these two parameters follow different trends, which is logic since their impact is different on the objective function. Thus, while the exportable energy is expected to impact positively, the energy that must be supplied from collective assets will force to more profusely exploit the collective generators and storage assets, eventually incurring in more costs.

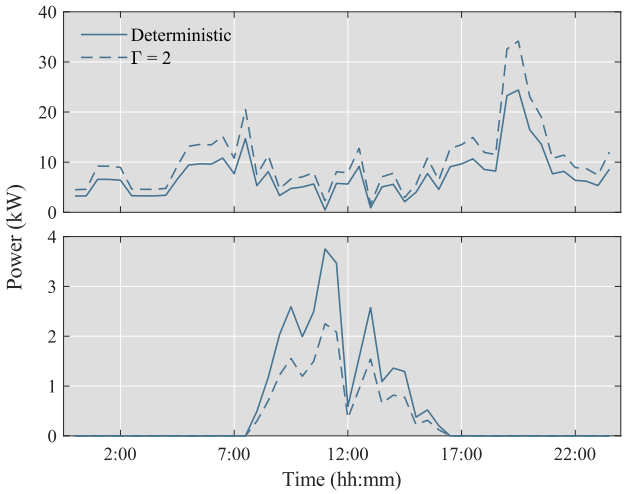

Fig. 9 - To-be-purchased (top) and exportable (bottom) powers drawn for stage 2

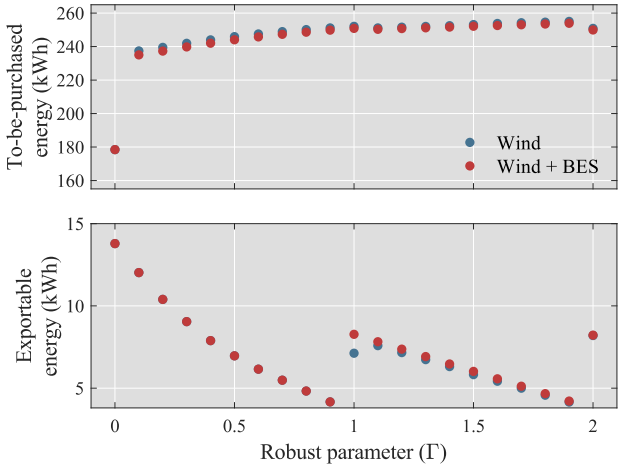

Fig. 10 - Total to-be-purchased and exportable energy for various values of the robust parameter (blue dots in this figure are often not visible due to the results obtained in such cases match with the value represented by red dots)

The results reported in Fig. 10 may suppose stressful conditions for collective assets, that may eventually hit their operability limits. Indeed, if the peak power that must be supplied surpasses the rated power of wind turbines, this energy could be supplied by batteries. This circumstance is clearly observed in Fig. 11. As observed, in case of only deploying wind turbines, the system is only fully supplied during the central hours through PV generation since the wind generators are not able to cover the demand. The situation is expected to be more critical as the robust parameter grows since, as seen in Fig. 11, the peak power is incremented by approximately 10 kW. This situation is partially solved by deploying batteries. These devices can exploit exportable and surplus wind energies, especially during evening, to be charged. The stored energy can be exploited throughout the day (e.g. at noon) to reduce the amount of unserved energy. These results are better appreciable in Fig. 12, where the total unserved energy is plotted for various values of Γ. As expected, this parameter grows with the robust parameter, being incremented by 39%. The non-served energy is also higher in case of only deploying wind turbines without storage capacity (+20%). In Fig. 12, the wind potential exploitation is also reported. This parameter follows the same trend, observing an increment of 25%. This is due to, as the energy required from prosumers grows, wind turbines have to be

operated at higher powers, eventually close or beyond their limits. It is also interesting to see that wind potential exploitation is considerably higher in case of deploying storage capacity (+12%). This is due to, as explained, BESs allow a more efficient use of wind energy, allowing to store eventual surplus generation which, otherwise, should be dissipated and therefore wasted.

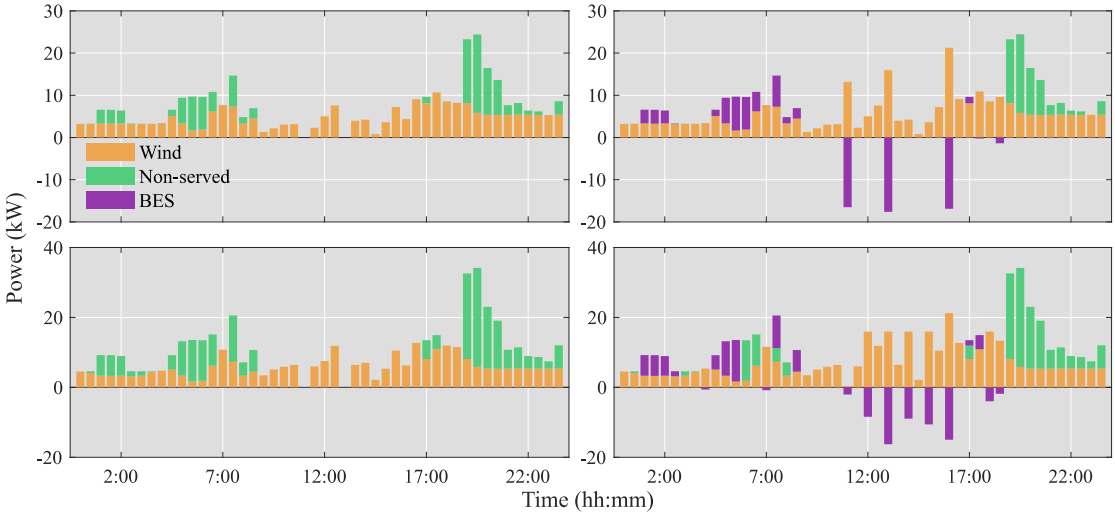

Fig. 11 - Scheduling result at stage 3 with deterministic conditions (top) or $\Gamma = 2$ (bottom) for the cases 'Wind' (left) or 'Wind+BES' (right)

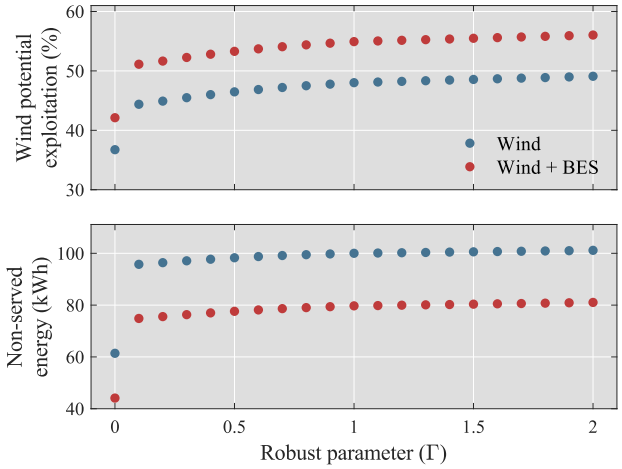

Fig. 12 - Wind potential exploitation and non-served energy for various values of the robust parameter

5.3 - Impact of the number of prosumers

The original case study encompasses six prosumers within a so-considered small-scale EC. However, the casuistry in this sense is wide and this section aims at providing an overview on the impact of the number of prosumers. To this end, the size of the original

community is enlarged by adding new peers, whose characteristics were randomly mimetic from the original prosumers described in Section 5.1. In order to keep provide a fair comparison, the installed wind power and storage capacity are incremented by 5% for each new prosumer. Intuitively, if more prosumers partake in the community, the surplus PV energy should increase, facilitating the energy saving through P2P processes. This aspect is studied in Fig. 13, where the total energy saving is compared for different number of prosumers. As seen, the total energy saved increases with the number of prosumers, however, this growth is not homogeneous and depends on the characteristics of each new prosumer incorporated to the community. This result strengthens the idea of optimally incorporating prosumers within existing communities, which will be studied in future works.

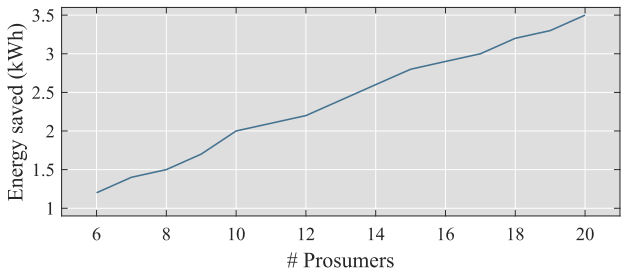

Fig. 13 - Total energy saved through P2P mechanism depending on the number of prosumers

Other critical aspect is the total time consumption depending on the total number of prosumers. Experiments performed by the authors showed an exponential increment of the computational time from 5-7 minutes in the original case to more than 45 minutes with 20 prosumers. This computational explosion is due to the cost of the first stage, which must be solved as many times as prosumers partake in the community. However, this does not suppose a critical issue for the practical implementation of the developed framework due to the following reasons:

- In real cases, the 1st stage is not solved sequentially. Instead, each prosumer solves his own HEM problem and only the stages 2 and 3 are performed by the

community operator. In this regard, the computational time is independent on the number of prosumers, just marginally varying with the community size.

- In the particular case in which the operator manages the individual resources, the 1st stage of the developed framework presents a highly parallelizable structure, which would help to reduce the computational effort notably. Moreover, the MILP structure of the developed framework ensures its good scalability to larger problems [71].

5.4 - Influence of the time step

In previous experiments, the time step has been taken equal to 30-min, which is considered reasonable for day-ahead scheduling problems [72]. However, some particular cases may require higher time resolution (e.g. in the presence of fast response units). Although this case is not usual, we provide in Fig. 14 a comparison of the total computation time for various time resolutions. As expected, the total computational time grows exponentially to the point to become unsolvable when taking time intervals shorter than 3-min. This is due to the variable-space size inversely grow with the time step, resulting in very large problems involving a large number of variables. As commented, this aspect is not considered critical as time slots shorter than 15-min are rarely used in this kind of applications. Nevertheless, high level computational languages like C or C++ could be used to speed up the computational time.

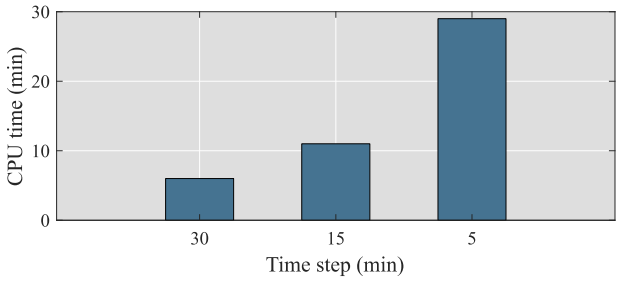

Fig. 14 - Total CPU time depending on the value of the time step

5.5 - Comparison with fully stochastic approach

There is a wide variety of uncertainty models available in the literature. However, maybe the simplest and most widely used is the stochastic programming and its variants. This modelling was already explained and has been used in this paper to represent the uncertain character of the wind speed. However, this same approach can be used to model the prosumers' net demand. To provide a fair comparison, we modelled the prosumers' net demand using the yearly data collected in [69]. These data allow us to represent the prosumers' demand via scenarios, being applied to the benchmark six-prosumer community studied in Section 5.2. Fig. 15 plots a comparison of the final objective function using fully-stochastic approach and the proposed hybrid framework for two values of the robust parameter. As observed, the objective function calculated with the stochastic model differs to those obtained with the proposed approach. This is due to, while the stochastic programming calculates a balanced result among all the scenarios considered, the RO seeks for extreme cases, as noted in [16]. Nevertheless, the level of robustness considered in RO is strongly influenced by the value of the robust parameter, as discussed previously.

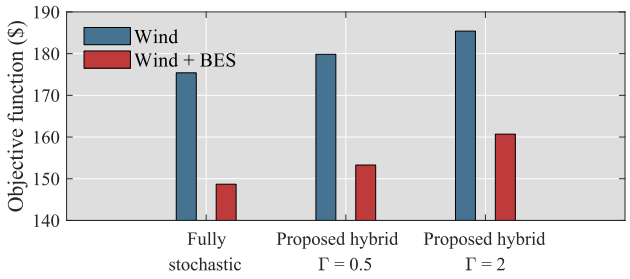

Fig. 15 - Total operational cost comparison between the proposed model and fully stochastic approach

Thus, maybe the major limitation of the developed approach is the necessity of estimating the prosumers' net demand with day-ahead accuracy. Nevertheless, within the proposed framework, each consumer is responsible of this task, being possible to impose penalty terms if a peer overestimates his surplus energy. Moreover, it is worth mentioning

that the developed hybrid proposal presents various advantages with respect fully stochastic models:

- The lack of historical data or proper models may difficult the treatment of the prosumers' net demand as a stochastic parameter.
- Privacy concerns limit the information exchanged between the peers and EC operator, for whom may be difficult infer proper stochastic models for the individual consumption of each prosumer.
- The prosumers' net demand can critically vary each day and is subjected to seasonal and daily cycles which might hinder the possibility of treating them as stochastic phenomena.
- The proposed hybrid framework is able to calculate extreme values and their corresponding scheduling plan, whose information may be very valuable for the community operator. In contrast, this information is missed when using stochastic approaches.

6 - Conclusions and future works

A new uncertainty modelling for isolated energy communities involving collective assets has been developed. The new proposal is based on hybridizing the conventional stochastic programming with robust optimization in a novel way, by which prosumers' net demand is treated using robust optimization while wind speed is handled via scenarios. The resulting optimization problem is arranged in a three-stage methodology, being each step responsible of individual home energy management problems, energy exchanges among prosumers and collective assets scheduling.

Results revealed the effectiveness of the developed formulation, obtaining coherent results in an acceptable computational time. A profuse comparison has been performed for different number of prosumers and time steps, revealing the scalability of the new

proposal thanks to its MILP character. In addition, a comparison with fully stochastic approaches has been also conducted, concluding that the developed hybrid method is more practical and replicable than fully stochastic approaches.

A case study on a six-prosumer benchmark community has been analysed. Results revealed the importance of collective assets and P2P process in collective supplying the prosumers' demand. In this sense, batteries played a vital role, helping to reduce the total unserved energy and operating cost by 20% and 19%, respectively, as well as enabling a more efficient use of wind energy. The impact of robustness has been also studied. In this case, the degree of robustness allows to consider unfavourable profiles, incrementing the expected importable energy by 28% compared to the deterministic case, while the exportable energy from prosumers is notably reduced by 40%. However, this consideration is achieved at expenses of expecting more monetary expenditures, in particular, the operating cost was incremented by 37%.

Future works will be focused on developing planning tools for isolated energy communities as well as new models for optimal integration of prosumers in collective structures such as communities or virtual power plants.

Acknowledgments

The icons used throughout this paper were developed by Triangle Squad, Uniconlabs, Victoruler, Didin jpr, dDara, Vitaly Gorbachev and verry purnomo, from www.flaticon.com.

References

[1] J. Teh, C.-M. Lai, Y.-H. Cheng. Impact of the Real-Time Thermal Loading on the Bulk Electric System Reliability. *IEEE Transactions on Reliability* 2017; 66(4): 1110-9. https://doi.org/10.1109/TR.2017.2740158.

[2] J. Teh. Uncertainty Analysis of Transmission Line End-of-Life Failure Model for Bulk Electric System Reliability Studies. *IEEE Transactions on Reliability* 2018; 67(3): 1261-8. https://doi.org/10.1109/TR.2018.2837114.

[3] M.K. Metwaly, J. Teh. Optimum Network Ageing and Battery Sizing for Improved Wind Penetration and Reliability. *IEEE Access* 2020; 8: 118603-11. https://doi.org/10.1109/ACCESS.2020.3005676.

[4] J. Teh, I. Cotton. Reliability Impact of Dynamic Thermal Rating System in Wind Power Integrated Network. *IEEE Transactions on Reliability* 2016; 65(2): 1081-9. https://doi.org/10.1109/TR.2015.2495173.

[5] C.-M. Lai, J. Teh. Comprehensive review of the dynamic thermal rating system for sustainable electrical power systems. *Energy Reports* 2022; 8: 3263-88. https://doi.org/10.1016/j.egyr.2022.02.085.

[6] K. Kusakana, S. Tangwe. Evaluating thermal dynamics of air to water heat pump due to stratification: Experiment and modelling. *Energy Reports* 2022; 8: 1118-25. https://doi.org/10.1016/j.egyr.2021.11.154.

[7] M. Alves, R. Segurado, M. Costa. On the road to 100% renewable energy systems in isolated islands. *Energy* 2020; 198: 117321. https://doi.org/10.1016/j.energy.2020.117321.

[8] Z.B. Medić, B. Ćosić, N. Duić. Sustainability of remote communities: 100% renewable island of Hvar. *Journal of Renewable & Sustainable Energy* 2013; 5(4): 041806. https://doi.org/10.1063/1.4813000.

[9] J. Teh, C.-M. Lai. Reliability impacts of the dynamic thermal rating and battery energy storage systems on wind-integrated power networks. *Sustainable Energy, Grids & Networks* 2019; 20: 100268. https://doi.org/10.1016/j.segan.2019.100268.

[10] F. Mohamad, J. Teh, C.-M. Lai. Optimum allocation of battery energy storage systems for power grid enhanced with solar energy. *Energy* 2021; 223: 120105. https://doi.org/10.1016/j.energy.2021.120105.

[11] J. Wang, H. Zhong, Z. Ma, Q. Xia, C. Kang. Review and prospect of integrated demand response in the multi-energy system. *Applied Energy* 2017; 202: 772-82. https://doi.org/10.1016/j.apenergy.2017.05.150.

[12] G. Iazzolino, N. Sorrentino, D. Menniti, A. Pinnarelli, M. De Carolis, L. Mendicino. Energy communities and key features emerged from business models review. *Energy Policy* 2022; 165: 112929. https://doi.org/10.1016/j.enpol.2022.112929.

[13] D. de São José, P. Faria, Z. Vale. Smart energy community: A systematic review with metanalysis. *Energy Strategy Reviews* 2021; 36: 100678. https://doi.org/10.1016/j.esr.2021.100678.

[14] International Energy Agency. Access to electricity. Online, available at: https://www.iea.org/reports/sdg7-data-and-projections/access-to-electricity, accessed May 25, 2022.

[15] A. Akbari-Dibavar, B. Mohammadi-Ivatloo, K. Zare, A. Anvari-Moghaddam. Optimal Scheduling of a Self-Healing Building Using Hybrid Stochastic-Robust Optimization Approach. *IEEE Transactions on Industry Applications* 2022; 58(3): 3217-26. https://doi.org/10.1109/TIA.2022.3155585.

[16] M. Tostado-Véliz, S. Kamel, F. Aymen, A.R. Jordehi, F. Jurado. A Stochastic-IGDT model for energy management in isolated microgrids considering failures and demand response. *Applied Energy* 2022; 317: 119162. https://doi.org/10.1016/j.apenergy.2022.119162.

[17] K. Kusakana. Optimal peer-to-peer energy sharing between grid-connected prosumers with different demand profiles and renewable energy sources. *IET Smart Grid* 2021; 4(3): 270-83. https://doi.org/10.1049/stg2.12027.

[18] A. Aminlou, B. Mohammadi-Ivatloo, K. Zare, R. Razzaghi, A. Anvari-Moghaddam. Peer-to-peer decentralized energy trading in industrial town considering central shared energy storage using alternating direction method of multipliers algorithm. *IET Renewable Power Generation* 2022; Early access. https://doi.org/10.1049/rpg2.12490.

[19] X. Liu, Z. Yan, J. Wu. Optimal coordinated operation of a multi-energy community considering interactions between energy storage and conversion devices. *Applied Energy* 2019; 248: 256-73. https://doi.org/10.1016/j.apenergy.2019.04.106.

[20] S. Lilla, C. Orozco, A. Borghetti, F. Napolitano, F. Tossani. Day-Ahead Scheduling of a Local Energy Community: An Alternating Direction Method of Multipliers Approach. *IEEE Transactions on Power Systems* 2020; 35(2): 1132-42. https://doi.org/10.1109/TPWRS.2019.2944541.

[21] B. Yan, M. Di Somma, G. Graditi, P.B. Luh. Markovian-based stochastic operation optimization of multiple distributed energy systems with renewables in a local energy community. *Electric Power Systems Research* 2020; 186: 106364. https://doi.org/10.1016/j.epsr.2020.106364.

[22] Z. Liu et al. Two-phase collaborative optimization and operation strategy for a new distributed energy system that combines multi-energy storage for a nearly zero energy

community. *Energy Conversion & Management* 2021; 230: 113800. https://doi.org/10.1016/j.enconman.2020.113800.

[23] H.-C. Jo, G. Byeon, J.-Y. Kim, S.-K. Kim. Optimal Scheduling for a Zero Net Energy Community Microgrid With Customer-Owned Energy Storage Systems. *IEEE Transactions on Power Systems* 2021; 36(3): 2273-80. https://doi.org/10.1109/TPWRS.2020.3036077.

[24] B.V. Rao et al. Optimal capacity management applied to a low voltage distribution grid in a local peer-to-peer energy community. *International Journal of Electrical Power & Energy Systems* 2022; 134: 107355. https://doi.org/10.1016/j.ijepes.2021.107355.

[25] A. Cosic, M. Stadler, M. Mansoor, M. Zellinger. Mixed-integer linear programming based optimization strategies for renewable energy communities. *Energy* 2021; 237: 121559. https://doi.org/10.1016/j.energy.2021.121559.

[26] Z. Liu et al. A novel distributed energy system combining hybrid energy storage and a multi-objective optimization method for nearly zero-energy communities and buildings. *Energy* 2022; 239(Part E): 122577. https://doi.org/10.1016/j.energy.2021.122577.

[27] C. Orozco, A. Borghetti, B. De Schutter, F. Napolitano, G. Pulazza, F. Tossani. Intra-day scheduling of a local energy community coordinated with day-ahead multistage decisions. *Sustainable Energy, Grids & Networks* 2022; 29: 100573. https://doi.org/10.1016/j.segan.2021.100573.

[28] A.D. Mustika, R. Rigo-Mariani, V. Debusschere, A. Pachurka. A two-stage management strategy for the optimal operation and billing in an energy community with collective self-consumption. *Applied Energy* 2022; 310: 118484. https://doi.org/10.1016/j.apenergy.2021.118484.

[29] Z. Liu et al. Co-optimization of a novel distributed energy system integrated with hybrid energy storage in different nearly zero energy community scenarios. *Energy* 2022; 247: 123553. https://doi.org/10.1016/j.energy.2022.123553.

[30] A. Mansour-Saatloo et al. Robust decentralized optimization of Multi-Microgrids integrated with Power-to-X technologies. *Applied Energy* 2021; 304: 117365. https://doi.org/10.1016/j.apenergy.2021.117635.

[31] European Commission. A European Green Deal. Online, available at: https://ec.europa.eu/info/strategy/priorities-2019-2024/european-green-deal_en, accessed May 26, 2022.

[32] S. Acharya. Analytic assessment of renewable potential in Northeast India and impact of their exploitation on environment and economy. *Environmental Science & Pollution Research* 2022; 29: 29704-18. https://doi.org/10.1007/s11356-022-18498-3.

[33] M.S. Javadi et al. Self-scheduling model for home energy management systems considering the end-users discomfort index within price-based demand response programs. *Sustainable Cities & Society* 2021; 68: 102792. https://doi.org/10.1016/j.scs.2021.102792.

[34] A.G. Gonzalez-Rodríguez, J. Serrano-Gonzalez, M. Burgos-Payan, J. Riquelme-Santos. Multi-objective optimization of a uniformly distributed offshore wind farm considering both economic factors and visual impact. *Sustainable Energy Technologies & Assessments* 2022; 52(part B): 102148. https://doi.org/10.1016/j.seta.2022.102148.

[35] M. Tostado-Véliz, S. Mouassa, F. Jurado. A MILP framework for electricity tariff-choosing decision process in smart homes considering 'Happy Hours' tariffs. *International Journal of Electrical Power & Energy Systems* 2021; 131: 107139. https://doi.org/10.1016/j.ijepes.2021.107139.

[36] L. Yan, X. Chen, Y. Chen. A consensus-based privacy-preserving energy management strategy for microgrids with event-triggered scheme. *International Journal of Electrical Power & Energy Systems* 2022; 141: 108198. https://doi.org/10.1016/j.ijepes.2022.108198.

[37] M. Collotta, G. Pau. A Solution Based on Bluetooth Low Energy for Smart Home Energy Management. *Energies* 2015; 8(10): 11916-38. https://doi.org/10.3390/en81011916.

[38] M. Elnour et al. Neural network-based model predictive control system for optimizing building automation and management systems of sports facilities. *Applied Energy* 2022; 318: 119153. https://doi.org/10.1016/j.apenergy.2022.119153.

[39] N.G. Paterakis, O. Erdinç, A.G. Bakirtzis, J.P.S. Catalão. Optimal Household Appliances Scheduling Under Day-Ahead Pricing and Load-Shaping Demand Response Strategies. *IEEE Transactions on Industrial Informatics* 2015; 11(6): 1509-19. https://doi.org/10.1109/TII.2015.2438534.

[40] M. Shafie-Khah, P. Siano. A Stochastic Home Energy Management System Considering Satisfaction Cost and Response Fatigue. *IEEE Transactions on Industrial Informatics* 2018; 14(2): 629-38. https://doi.org/10.1109/TII.2017.2728803.

[41] S. Mandal, B.K. Das, N. Hoque. Optimum sizing of a stand-alone hybrid energy system for rural electrification in Bangladesh. *Journal of Cleaner Production* 2018; 200: 12-27. https://doi.org/10.1016/j.jclepro.2018.07.257.

[42] M. Tostado-Véliz, S. Gurung, F. Jurado. Efficient Solution of Many-objective Home Energy Management Systems. *International Journal of Electrical Power & Energy Systems* 2022; 136: 107666. https://doi.org/10.1016/j.ijepes.2021.107666.

[43] M. Tostado-Véliz, M. Bayat, F. Jurado. Home energy management in off-grid dwellings: Exploiting flexibility of thermostatically controlled appliances. *Journal of Cleaner Production* 2021; 310: 127507. https://doi.org/10.1016/j.jclepro.2021.127507.

[44] F. Garcia-Torres, D.G. Vilaplana, C. Bordons, P. Roncero-Sánchez, M.A. Ridao. Optimal Management of Microgrids With External Agents Including Battery/Fuel Cell Electric Vehicles. *IEEE Transactions on Smart Grid* 2019; 10(4): 4299-308. https://doi.org/10.1109/TSG.2018.2856524.

[45] S. Wang, S. Yuan. Interval optimization for integrated electrical and natural-gas systems with power to gas considering uncertainties. *International Journal of Electrical Power & Energy Systems* 2020; 119: 105906. https://doi.org/10.1016/j.ijepes.2020.105906.

[46] S. Zeinal-Kheiri, A.M. Shotorbani, A. Khardenavis, B. Mohammadi-Ivatloo, R. Sadiq, K. Hewage. An adaptive real-time energy management system for a renewable energy-based microgrid. *IET Renewable Power Generation* 2021; 15(13): 2918-30. https://doi.org/10.1049/rpg2.12223.

[47] M.F. Elmorshedy, M.R. Elkadeem, K.M. Kotb, I.B.M. Taha, D. Mazzeo. Optimal design and energy management of an isolated fully renewable energy system integrating batteries and supercapacitors. *Energy Conversion & Management* 2021; 245: 114584. https://doi.org/10.1016/j.enconman.2021.114584.

[48] M.M. Kama, I. Ashraf, E. Fernandez. Optimal planning of renewable integrated rural microgrid for sustainable energy supply. *Energy Storage* 2022; 4(4): e332. https://doi.org/10.1002/est2.332.

[49] M. Elnour et al. Performance and energy optimization of building automation and management systems: Towards smart sustainable carbon-neutral sports facilities. *Renewable & Sustainable Energy Reviews* 2022; 162: 112401. https://doi.org/10.1016/j.rser.2022.112401.

[50] I. Alsaidan, A. Khodaei, W. Gao. A Comprehensive Battery Energy Storage Optimal Sizing Model for Microgrid Applications. *IEEE Transactions on Power Systems* 2018; 33(4): 3968-80. https://doi.org/10.1109/TPWRS.2017.2769639.

[51] F. Jalilian, M.A. Mirzaei, K. Zare, B. Mohammadi-Ivatloo, M. Marzband, A. Anvari-Moghaddam. Multi-energy microgrids: An optimal despatch model for water-energy nexus. *Sustainable Cities & Society* 2022; 77: 103573. https://doi.org/10.1016/j.scs.2021.103573.

[52] M. Tostado-Véliz, P. Arévalo, F. Jurado. An optimization framework for planning wayside and on-board hybrid storage systems for tramway applications. *Journal of Energy Storage* 2021; 43: 103207. https://doi.org/10.1016/j.est.2021.103207.

[53] C. Feng, F. Wen, S. You, Z. Li, F. Shahnia, M. Shahidehpour. Coalitional Game-Based Transactive Energy Management in Local Energy Communities. *IEEE Transactions on Power Systems* 2020; 35(3): 1729-40. https://doi.org/10.1109/TPWRS.2019.2957537.

[54] C.-M. Lai, J. Teh. Network topology optimisation based on dynamic thermal rating and battery storage systems for improved wind penetration and reliability. *Applied Energy* 2022; 305: 117837. https://doi.org/10.1016/j.apenergy.2021.117837.

[55] M.K. Metwaly, J. Teh. Probabilistic Peak Demand Matching by Battery Energy Storage Alongside Dynamic Thermal Ratings and Demand Response for Enhanced Network Reliability. *IEEE Access* 2020; 8: 181547-59. https://doi.org/10.1109/ACCESS.2020.3024846.

[56] Z. Liu, P. Jiang, L. Zhang, X. Niu. A combined forecasting model for time series: Application to short-term wind speed forecasting. *Applied Energy* 2020; 259: 114137. https://doi.org/10.1016/j.apenergy.2019.114137.

[57] M. Vahid-Ghavidel et al. Novel Hybrid Stochastic-Robust Optimal Trading Strategy for a Demand Response Aggregator in the Wholesale Electricity Market. *IEEE Transactions on Industry Applications* 2021; 57(5): 5488-98. https://doi.org/10.1109/TIA.2021.3098500.

[58] J.R. Birge, F. Louveaux. *Introduction to Stochastic Programming*. Berlin: Springer; 2011.

[59] M. Mahdavi, H.H. Alhelou, M.R. Hesamzadeh. An Efficient Stochastic Reconfiguration Model for Distribution Systems With Uncertain Loads. *IEEE Access* 2022; 10: 10640-52. https://doi.org/10.1109/ACCESS.2022.3144665.

[60] H. Rashidizadeh-Kermani, M. Vahedipour-Dahraie, A. Anvari-Moghaddam, J.M. Guerrero. A stochastic bi-level decision-making framework for a load-serving entity in day-ahead and balancing markets. *International Transactions on Electrical Energy Systems* 2019; 29(11): e12109. https://doi.org/10.1002/2050-7038.12109.

[61] Z. Pourmirza, S. Walker, J. Brooke. Data reduction algorithm for correlated data in the smart grid. *IET Smart Grid* 2021; 4(5): 474-88. https://doi.org/10.1049/stg2.12010.

[62] A. García-Cerezo, L. Baringo, R. García-Bertrand. Representative days for expansion decisions in power systems. *Energies* 2020; 13: 335, https://doi.org/10.3390/en13020335.

[63] E.S. Pinto, L.M. Serra, A. Lázaro. Evaluation of methods to select representative days for the optimization of polygeneration systems. Renewable Energy 2020; 151: 488–502, https://doi.org/10.1016/j.renene.2019.11.048.

[64] M. Tostado-Véliz, S. Kamel, H.M. Hasanien, R.A. Turky, F. Jurado. A mixed-integer-linear-logical programming interval-based model for optimal scheduling of isolated microgrids with green hydrogen-based storage considering demand response. *Journal of Energy Storage* 2022; 48: 104028. https://doi.org/10.1016/j.est.2022.104028.

[65] D. Bertsimas, M. Sim. The Price of Robustness. *Operations Research* 2004; 52(1): 35-53. https://doi.org/10.1287/opre.1030.0065.

[66] D. Bertsimas, M. Sin. Robust discrete optimization and network flows. *Mathematical Programming* 2003; 98: 49-71. https://doi.org/10.1007/s10107-003-0396-4.

[67] Gurobi Optimization L.L.C. Gurobi Optimizer Reference Manual, 2021. Online, available at: https://www.gurobi.com, accessed May 27, 2022.

[68] National Centers for Environmental Information. Land-based datasets and products. Online, available at: https://www.ncei.noaa.gov/products/land-based-station, accessed May 27, 2022.

[69] T. Singh. Smart home dataset with weather information. Online, available at: https://www.kaggle.com/datasets/taranvee/smart-home-dataset-with-weather-information, accessed May 27, 2022.

[70] M. Tostado-Véliz, S. Kamel, H.M. Hasanien, P. Arévalo, R.A. Turky, F. Jurado. A stochastic-interval model for optimal scheduling of PV-assisted multi-mode charging stations. *Energy* 2022; 253: 124219. https://doi.org/10.1016/j.energy.2022.124219.

[71] M. Jooshaki, H. Farzin, A. Abbaspour, M. Fotuhi-Firuzabad, M. Lehtonen. A Model for Stochastic Planning of Distribution Network and Autonomous DG Units. *IEEE Transactions on Industrial Informatics* 2020; 16(6): 3685-96. https://doi.org/10.1109/TII.2019.2936280.

[72] M. Salgado, M. Negrete-Pincetic, Á. Lorca, D. Olivares. A low-complexity decision model for home energy management systems. *Applied Energy* 2021; 294: 116985. https://doi.org/10.1016/j.apenergy.2021.116985.